

UNCLASSIFIED

AD NUMBER

AD274314

NEW LIMITATION CHANGE

TO

**Approved for public release, distribution
unlimited**

FROM

**Distribution authorized to U.S. Gov't.
agencies and their contractors;
Administrative/Operational Use; 16 MAR
1962. Other requests shall be referred to
National Aeronautics and Space
Administration, Washington, DC.**

AUTHORITY

NASA TR Server website

THIS PAGE IS UNCLASSIFIED

UNCLASSIFIED

AD. 274 314

*Reproduced
by the*

**ARMED SERVICES TECHNICAL INFORMATION AGENCY
ARLINGTON HALL STATION
ARLINGTON 12, VIRGINIA**



UNCLASSIFIED

NOTICE: When government or other drawings, specifications or other data are used for any purpose other than in connection with a definitely related government procurement operation, the U. S. Government thereby incurs no responsibility, nor any obligation whatsoever; and the fact that the Government may have formulated, furnished, or in any way supplied the said drawings, specifications, or other data is not to be regarded by implication or otherwise as in any manner licensing the holder or any other person or corporation, or conveying any rights or permission to manufacture, use or sell any patented invention that may in any way be related thereto.

Technical Report No. 32-238

An Experimental Investigation of a Gas-Particle System

Robert Sehgal



474200

JET PROPULSION LABORATORY
CALIFORNIA INSTITUTE OF TECHNOLOGY
PASADENA, CALIFORNIA

March 16, 1962

NO OTS

NATIONAL AERONAUTICS AND SPACE ADMINISTRATION
CONTRACT NO. NAS 7-100

Technical Report No. 32-238

**An Experimental Investigation of a
Gas-Particle System**

Robert Sehgal

L. R. Piasecki
L. R. Piasecki, Chief
Solid Propellant Engineering

JET PROPULSION LABORATORY
CALIFORNIA INSTITUTE OF TECHNOLOGY
PASADENA, CALIFORNIA

March 16, 1962

CONTENTS

I. Introduction	1
A. Motor Exhaust Collection	2
B. Propellant	3
C. Motor Configuration	3
D. Nozzle Configurations	3
E. Igniters	3
II. Particle Collection	4
III. Particle Analysis Techniques	5
A. Micromerograph	5
B. MSA Centrifuge	5
C. Coulter Counter	5
D. Electron Microscopic Analysis	5
1. Sample Preparation for Electron Microscopy	5
2. Electron Micrographs	6
3. Particle Size Analysis and Method of Data Reduction	6
IV. Discussion of Results	6
A. Pressure Effect on Particle Size	6
B. Particle Diameter-Pressure Relationship	7
C. Effect of Nozzle Convergent Section on Particle Size	7
D. Effect of Increased Particle Residence Time in Chamber	8
E. Effect of Aluminum Percent in Propellant on Particle Size	8
F. Effect of Aluminum Particle Size in Propellant on Exhaust Particle Size	8
G. Effect of Combustion Temperature on Aluminum Oxide Particles	9
H. Discussion of Extremely Small Particles	9
V. Chemical Analysis	10
VI. Summary of Results	11

FIGURES

1. Stainless steel collection tank	2
2. 5 X 6 rocket motor mounted on flange cover plate	3
3. Aft portion of stainless steel collection tank after firing	4
4. Forward portion of collection tank after firing	4
5. Micrograph of aluminum oxide sample obtained from motor firing at 1000-psi chamber pressure	12
6. Micrograph of aluminum oxide sample obtained from motor firing at 700-psi chamber pressure	13
7. Micrograph of aluminum oxide sample obtained from motor firing at 500-psi chamber pressure	14
8. Plot of percent greater than and percent total volume below vs particle size, of aluminum oxide sample obtained from motor firing at 500-psi chamber pressure	15
9. Micrograph of aluminum oxide sample obtained from motor firing at 365-psi chamber pressure	16
10. Micrograph of aluminum oxide sample obtained from motor firing at 277-psi chamber pressure	17
11. Plot of percent greater than and percent total volume below vs particle size, of aluminum oxide sample obtained from motor firing at 277-psi chamber pressure	18
12. Micrograph of aluminum oxide sample obtained from motor firing at 200-psi chamber pressure	19
13. Micrograph of aluminum oxide sample obtained from motor firing at 150-psi chamber pressure	20
14. Plot of percent greater than and percent total volume below vs particle size, of aluminum oxide sample obtained from motor firing at 150-psi chamber pressure	21
15. Micrograph of aluminum oxide sample obtained from motor firing at 75-psi chamber pressure	22
16. Another micrograph of aluminum oxide sample obtained from motor firing at 75-psi chamber pressure	23
17. Plot of chamber pressure vs average particle size by volume	24
18. Micrograph of aluminum oxide sample obtained from motor firing at 150-psi chamber pressure and without any nozzle (micrograph supplied by Aeronutronics, a Division of Ford Motor Company)	25

ABSTRACT

It has been shown that the presence of particles in the gas flow through rocket nozzles results in appreciable performance degradation,¹ which tends to cancel the increased performance that results from high combustion temperatures of propellants with metal additives. The higher the particle weight fraction, the lower the efficiency (delivered I_{sp} /theoretical I_{sp}). In addition to the above, the results of theoretical investigations indicate that performance losses increase appreciably with increased particle sizes. The presence of very small particles is least detrimental as they cause the least reduction in performance due to the fact that these particles have a high aerodynamic drag-to-mass ratio and thus high acceleration and velocity. Small particles have velocities and temperatures throughout the nozzle that are almost equal to those of the gas; however, the gas velocity itself may be somewhat reduced by the small particles.

Results of extensive experimental investigations and the effect of pertinent parameters on particle size distribution, particle shape, and combustion efficiency are discussed. With aluminized propellants, it is shown that particle size distribution is pressure-dependent. An empirical relationship giving the average particle diameter D on a volume basis as a function of the pressure P is developed, which is written as

$$\log P = a + bD$$

¹R. F. Hoglund, *Recent Advances in Gas-Particle Nozzle Flows*, Preprint No. 2331-62, presented at the ARS Solid Propellant Rocket Conference, Baylor University, Waco, Tex., January 24-26, 1962.

I. INTRODUCTION

Since the only direct, and most effective, means of overcoming performance losses associated with lag effects is the use of a propellant system that produces small particles, a comprehensive experimental program was initiated at the Jet Propulsion Laboratory approximately one

year ago to determine the effect of the following parameters on particle size distribution:

1. Chamber pressure
2. Nozzle configuration

3. Particle residence time in chamber
4. Aluminum percentage in propellant
5. Aluminum particle size in propellant
6. Chamber temperature

The scope of the study also included chemical analysis of the collected samples and density determination of aluminum oxide particles.

Before any particle collection or analysis could be accomplished, several areas of investigation were necessary.

A. Motor Exhaust Collection

The technique commonly used to collect exhaust particles has been by placing glass or metal slides just out of the hottest portion of the rocket exhaust and allowing

particles to impinge upon these slides. This method was discarded because it was questionable that the limited sample collected in this manner was the actual representation and shape of the whole particle spectrum produced by the combustion process. Of the various other collection techniques investigated, the most effective was to construct a completely enclosed tank in which the motor is fired and all the exhaust products are collected. A corrosion study of various metal samples placed directly in the nozzle exhaust stream was conducted to determine the effect of highly corrosive exhaust products on various materials. Since pit corrosion occurred in most of the samples at the same rate, it was decided to use stainless steel 347 as the tank construction material because of its excellent weldability and low cost.

The stainless steel collection tank (shown in Fig. 1) is 8 ft. long, with an outside diameter of 42 in. and an inter-



Fig. 1. Stainless steel collection tank

nal volume of 75 ft³. The entire unit was mounted on wheels to facilitate disassembly. The inside surface was polished to a No. 4 finish. A large center flange allows the separation of the tank into two sections. Two 6-in. openings in the flange are provided for a safety blow-out disc, and vacuum and pressure attachments to the tank. The head end of the tank has a 10-in. flange opening. The motor is mounted on the threaded stud welded to the flange cover plate (see Fig. 2). O-ring seals were used on all flange openings.

B. Propellant

Polyurethane-type propellants containing 12, 16, and 20% aluminum were cast in small chambers. Two grades of aluminum, Alcoa 1230 ($\sim 15 \mu$) and MD-105 ($\sim 5 \mu$), were used in the propellants. Ballistic information was obtained by firing small charges at varying chamber pressures and grain designs.

C. Motor Configuration

For particle collection tests, a basic motor, 5 in. O.D. by 6 in. long, with a circular port and one end restricted, containing approximately 3.5 lb of propellant, was selected. With polyurethane propellants containing 12 and 18% aluminum, this configuration produced a nearly flat pressure-time curve, with a variation in pressure of less than 5% during the firing period. Moreover, there was a minimum of aluminum oxide coating on the convergent or throat section.

D. Nozzle Configurations

Two conditions making particle collection procedures extremely difficult were the high exit temperatures and velocities of the particles expelled from conventional nozzles. To alleviate these problems, a simple converging nozzle was designed with a 30-deg entrance angle and a molybdenum insert. High-speed photographs of motor exhaust characteristics, using the converging nozzles, revealed wide and rapid expansion of gaseous products upon exit from the nozzle, while the solid particulate matter remained in a fairly well defined center core. Two things were accomplished: (1) Lower initial particle velocity upon exit from the nozzle than with conventional converging-diverging nozzles was achieved. (2) Hot ex-

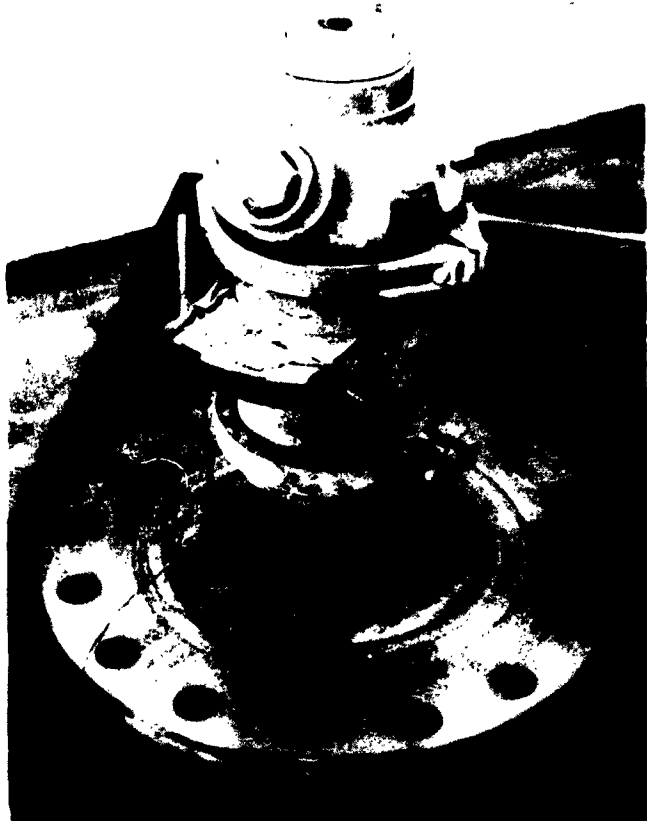


Fig. 2. 5 x 6 rocket motor mounted on flange cover plate

haust gases were rapidly diverged away from the particles, allowing impingement into ambient gases with resultant rapid cooling and velocity decrease.

E. Igniters

To eliminate the possible contamination of aluminum oxide with the metal oxides produced from commercially available igniters, two 2-g solid-propellant strips imbedded with light nichrome wires were placed diametrically opposite each other in the tubular grain and ignited with an 18-v battery source. Ignition with this method has proved excellent.

II. PARTICLE COLLECTION

For particle collection in the tank, the motor was mounted to the 10-in. blind flange cover plate and all flanges were closed and sealed. The air was evacuated from the tank (to approximately 3 mm Hg) and nitrogen was introduced to attain atmospheric conditions. Nitrogen was used to provide an inert atmosphere and to prevent any combustion of solids in the tank. After motor firing, a few minutes were allowed for tank pressure to settle. The excess gas was expelled slowly through a needle valve until atmospheric pressure was achieved. Then the remaining gas was slowly evacuated in order to avoid taking any solids from the tank. Dry nitrogen was introduced to regain atmospheric pressure, and the tank halves were separated. As shown in Fig. 3 and 4, the aluminum oxide had completely coated the tank walls. Evidently the water and organic liquids originat-

ing in the combustion process had condensed on the tank walls, and as the solid particles impinged or settled out, they mixed with this liquid. As the evacuation process occurred, the liquids boiled off, leaving the caked coating of dry aluminum oxide. The exhaust products were swept from the walls with a soft nylon brush. By careful and repeated brushings, up to 90% of the theoretical predicted solids were recovered. No evidence of particles sticking to the walls has ever been noticed, indicating that particles solidify before impingement on the tank walls.

All the samples collected from the tank were dried at 250°C for 24 hours to drive off impurities and volatiles without affecting the aluminum oxide particles. Coning and quartering sample techniques were used to provide representative samples for particle analysis.

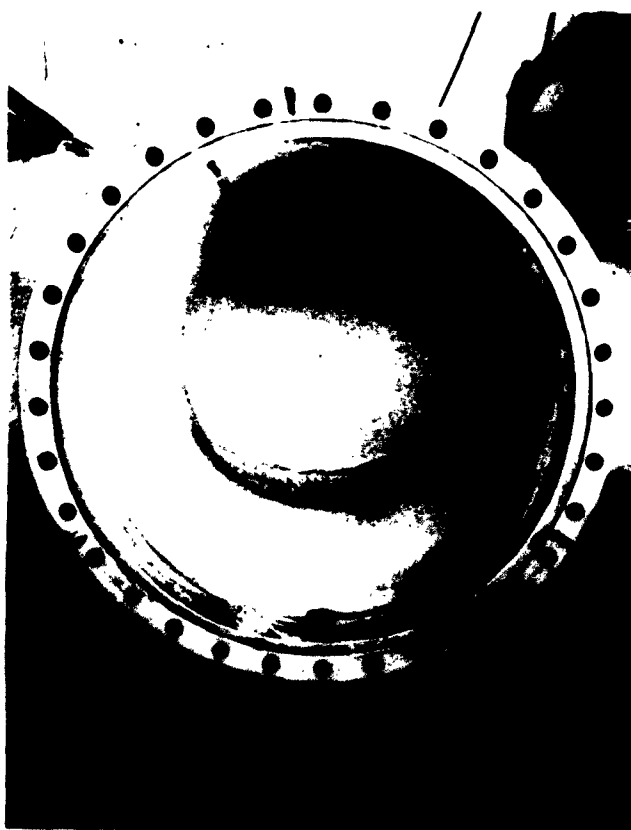


Fig. 3. Aft portion of stainless steel collection tank after firing



Fig. 4. Forward portion of collection tank after firing

III. PARTICLE ANALYSIS TECHNIQUES

Various techniques and equipment are commercially available for determining particle size distribution. Each technique has its inherent biases and limitations, and extreme care should be exercised in interpreting the results obtained from each type. The size range of the sample and data desired, either for direct interpretation or for subsequent representation of data and accuracy of operation, must be considered in selection of method of particle size measurement. Some of the methods investigated before the final selection are discussed in the following.

A. Micromerograph

Micromerograph results depend upon the cumulative weight on the sensitive balance pan at the bottom of a sedimentation column. A sample of less than 10μ , containing a large percentage of aluminum oxide particles, fired into the column resulted in a 50% loss of the sample to the column walls (even after treatment with an antistatic agent). The data obtained were not representative of the original sample, but only that part which reached the balance pan. Also, the lower limit of accuracy for the micromerograph is 2 to 3μ for aluminum oxide. For these reasons this method was discarded.

B. MSA Centrifuge

The MSA (Mine Safety Appliances Company) particle size analyzer consists of a calibrated centrifuge, reading projector, and centrifuge tubes with 0.75-mm-diam. capillary bores in the lower portion. Best results were obtained by using benzene as the sedimentation liquid and 50-50 mineral oil and Iso-octane as the feeding liquid. A small amount of sodium sulfonate was added to the feeding liquid as a dispersing agent. Approximately 1 g of particle sample is placed in 100 ml of feeding liquid and the mixture is stirred in a Waring blender for a few minutes. The feeding liquid has a 10% lower density than the benzene, so it floats on the benzene sedimentation liquid which fills the centrifuge tubes. As the particles settle through the benzene column under the action of the centrifugal field, they fill the capillary, where heights may then be read at predetermined times via the projector. Diameter calculations are based on Stoke's law, and different data sheets are compiled, relating particle size and centrifuge speed to time. The size distribution is obtained by dividing the height to which the capillary is filled at the desired time, hence particle diameter, by the total height after all particles have settled. This method

seems well suited for rapid analysis; however, because extreme difficulties were experienced in properly deagglomerating the particles and obtaining reproducible results, this technique was also discarded.

C. Coulter Counter

This method provides a rapid and reasonably accurate analysis based on particle volume. It is adaptable for analysis to particle sizes ranging from 0.6μ to over 200μ . By this technique, a suspension of particles in conductive liquid flows through an aperture with simultaneous flow of electric current, resulting in a series of electrical pulses, each pulse being proportional in magnitude to the volume of the particle causing it. The pulses are amplified, scaled, and counted to provide data for plotting cumulative frequency against particle size. The drawbacks to this method are limits in the region of lower sizes, and the lack of commercial firms well versed in the method. Data obtained on a few samples were used for comparative purposes.

D. Electron Microscopic Analysis

Of the methods considered, microscopic techniques, though time-consuming, were found to be the most reliable and accurate in particle size analysis. The electron microscope, which was most successful in analysis of particle shape, particle size distribution—especially in the submicron range—surface structure, porosity, etc., was the final selection for this investigation. All samples were analyzed by a commercial firm well qualified in the use of the electron microscope,² and good, reproducible results were obtained.

1. Sample Preparation for Electron Microscopy

Of several techniques which were tested to disperse the particles, the following process was finally used. Representative portions of each of the samples were placed in a mildly acidic electrolyte, formed with HCl and water, and after mechanical dispersion had progressed as far as possible, the samples were subjected to 40-kc agitation in an Acoustica ultrasonic vibrator for a period of five minutes. Aliquots of each specimen were placed on carbon-filmed electron microscope viewing grids, and after drying, the grids were viewed in a Norelco EM 100

²Sloan Research Industries, Santa Barbara, California

electron microscope. A minimum of four grids were viewed and studied for each sample.

2. Electron Micrographs

A group of micrographs taken of samples at various chamber pressures is shown at the end of this Report. While a minimum of four micrographs were made for each sample, only one representative micrograph per sample is shown. The scale shown in the lower right-hand corner of each of the micrographs represents a distance of 1μ on the surface of the micrograph. As the micrographs show, almost all particles are perfectly spherical in character. There appears to be a considerable amount of association between spheres. The nonspherical particles were assumed to be of no significance.

Surface replication studies performed in conjunction with particle size analysis on all the collected samples indicated that particle surfaces were smooth and continuous, with no pocks or pores in particles in the range of 0.3μ and above. From this, it may be concluded that particles were of high density and continuous.

3. Particle Size Analysis and Method of Data Reduction

Particle size analysis was accomplished through the use of an equivalent circle technique, which is well known in the particle size analysis field. In particular, for this study

all particles in the range of 0.1μ and above were counted on a minimum of four micrographs per sample. The following restrictions were placed on the particle count:

1. No particle was counted if the periphery of that particular particle extended beyond the boundaries of the micrograph.
2. All particles were assumed to be spherical in character.
3. No particle was counted unless a sufficient amount of its periphery could be delineated to permit the deduction of the particle diameter.
4. No particle below 0.1μ was evaluated in size, but these were included in the total particle count.

The particle size count below 0.4μ was made to estimate the total volume occupied by the particle in this range. The percent total count in each case was made as a normalized distribution of the particle count, expressed as a percent. The percent total volume was calculated as a normalized result of the product of the particle count and the cube of the diameter expressed as a percent. For each case a log-log plot of particle size vs percent population and particle size vs percent total volume was made. Some of these plots are included in the Figures at the end of this Report.

IV. DISCUSSION OF RESULTS

A. Pressure Effect on Particle Size

The basic 5×6 motors, containing identical propellant formulation and with a 30-deg nozzle entrance angle, were fired in the stainless steel tank at various chamber pressures. As mentioned earlier, these charges produced a nearly flat pressure-time curve. Collected samples were analyzed to determine the effect of chamber pressure on particle sizes. Motor firings in many cases were duplicated to determine the reproducibility of results obtained by electron microscopic analysis. The following discussion summarizes results of the analyses.

1. 1000-psi Chamber Pressure

Electron microscopic analysis of the aluminum oxide sample collected at 1000-psi chamber pressure indicated a complete absence of small or very fine particles. Some very large particles were present, the largest of those detected measuring about 30μ . The general character of the sample is indicated by the micrograph shown in Fig. 5. There was a wide distribution of moderate to large particles. For all practical purposes the size range was from 1 to 12μ . Average particle size on a volume basis was found to be approximately 4.7μ .

2. 700-psi Chamber Pressure

The general character of the sample obtained at 700-psi chamber pressure is shown by the micrograph in Fig. 6. Virtually no fine particles were present in this sample. There was a fairly even distribution of particles between 0.7- μ to about 9- μ range. On a volume basis the average particle size was approximately 4.1 μ .

3. 500-psi Chamber Pressure

The micrograph in Fig. 7 shows the general character of the aluminum oxide sampling at 500-psi chamber pressure. Figure 8 is a plot showing percent greater than size vs particle diameter and percent total volume occupied vs particle diameter. Some particles in the range of 10 μ were observed; however, the number of particles above 6 μ was extremely small. Volume contribution of particles below 0.7 μ was less than 1% of total volume, even though particles in the range of 0.4 μ accounted for almost 30% of total count. Large particles are, of course, of overwhelming importance on a volume basis. The percent total volume occupied vs particle diameter (Fig. 8) indicates an average particle size of about 3.5 μ .

4. 365-psi Chamber Pressure

In the sample obtained at 365-psi chamber pressure, wide distribution of large to moderately small particles was noted under the electron microscope. Maximum particle size was found to be about 6 μ , with a high concentration of particles in the 0.2- to 2.0- μ range. Roughly 7% of all particles were above 2 μ in size, having a fairly even distribution between 3 and 5 μ . Figure 9 shows the general character of the sample. On a volume basis, average particle size was found to be about 3.0 μ .

5. 277-psi Chamber Pressure

The micrograph in Fig. 10 shows that the number of large particles was very small in the sample of aluminum oxide obtained at 277-psi chamber pressure. Figure 11 shows a log-log plot of percent greater than size vs particle diameter and percent total volume vs particle size. Count plot fell below the 1% range at slightly above 2.5 μ , indicating that a significantly large number of small particles were present. Four times as many small particles were found below 0.4 μ as compared to the sample obtained at 500-psi chamber pressure. There was an extremely high population of particles in the range of 1.5 μ . Average particle size on a volume basis was found to be 2.5 μ .

6. 200-psi Chamber Pressure

An extremely large number of small particles were present in the sample obtained at 200-psi chamber pressure. There was a wide spectrum of particle size, ranging from submicron up to a particle size in the range of 3 μ . Contribution to the total volume was accounted for by particles of about 2 μ . Figure 12 shows a micrograph of this sample. Average particle size on a volume basis was found to be about 2.0 μ .

7. 150-psi Chamber Pressure

In the sample obtained at 150-psi chamber pressure, all the particles were basically in the submicron range. No particle was found to be above 2.5 μ . These characteristics are shown in Fig. 13. Figure 14 is a plot of percent greater than size and percent total volume vs particle diameter. On a volume basis, the average particle size was 1.5 μ .

8. 75-psi Chamber Pressure

As seen in Fig. 15 and 16, the sample at 75-psi chamber pressure contained virtually no intermediate or large size particles, but was comprised almost completely of extremely small particles in the submicron range.

B. Particle Diameter - Pressure Relationship

Results of the above particle size analyses clearly indicate that with aluminized propellants, particle size distribution is pressure-dependent. Lower chamber pressure results in smaller particle sizes and vice versa. In fact, all the motors fired at 100-psi chamber pressure or below resulted in aluminum oxide particles in the submicron range. By plotting chamber pressure P against average particle diameter D on a volume basis, a straight-line relationship is obtained on semilog scale, as shown in Fig. 17. Thus a new empirical relationship, giving the aluminum oxide particle diameter as a function of the pressure, can be written as

$$\log P = a + bD$$

C. Effect of Nozzle Convergent Section on Particle Size

To determine the effect of a convergent nozzle section on particle sizes, 5 \times 6 motors containing the same propellant formulation were fired in the collection tank, with and without the convergent nozzle section, at approximately the same chamber pressure (150 psi). In the latter

case, the tank was pressurized to the desired pressure level before ignition. For this series of tests, the upper limit of the chamber pressure was set at 170 psi to be well below the yield level of the stainless steel tank. Motor firings without any nozzle also yielded important information as to the size, shape, and density of aluminum oxide particles as they came out of the chamber. It was also possible to compare the combustion efficiency in the two cases, as discussed further in Section V.

Results of the particle size and chemical analysis indicate that essentially there was no difference between the two cases (with and without nozzle) with regard to the maximum or minimum sizes, character of the X-ray diffraction patterns, actual aluminum oxide density, and combustion efficiency. However, one pertinent result was obtained. In the case of motors fired without a nozzle, all the particles were basically in the submicron range due to lower chamber pressure, and no particles were found above 2.5 μ . In the case of motors fired with a 30-deg nozzle entrance angle and at the same chamber pressure, the distribution of particle sizes was essentially the same, except that on two out of the four viewing grids, one or two particles were found in the 4- μ range. This is probably due to the slight coating of aluminum oxide in the convergent section of the nozzle which sluffed through as large masses of agglomerated particles. This effect was also noted with charges fired below 100-psi chamber pressure with a 30-deg nozzle entrance angle, where all the particles were in the submicron range, except for one or two particles on one of the viewing grids which were in the 3- μ range. As the contraction ratio was increased—that is, going to a steeper entrance angle—the size of the agglomerated particles increased, indicating that extremely sharp nozzle entrance angles should be avoided, if possible. A micrograph of one of the viewing grids, for a sample without a nozzle, is shown in Fig. 13.

Because of their great interest in this project, Aeronomutronics³ was given a set of samples from these firings for their independent cross-check. A micrograph of one of their viewing grids is shown in Fig. 18. The findings of their analysis were in complete agreement with the results of the investigation at the Jet Propulsion Laboratory.

D. Effect of Increased Particle Residence Time in Chamber

In order to evaluate the effect on exhaust particle sizes of increased particle residence time in chamber, eight

charges (5 \times 6 motor) were cast in chambers 5 in. O.D. \times 10 in. long, where all the propellant was located on the forward end of the motor. Then 5 \times 6 and 5 \times 10 motors, containing the same propellant and with a 30-deg nozzle entrance angle, were fired in the tank at identical chamber pressures. The particle size analysis indicated that increased residence time in the chamber resulted in smaller particle sizes. For example, the results of particle size analysis on samples collected by firing motors at 200-psi chamber pressure indicated that there was a wide spectrum of particle sizes ranging from submicron particles up to a particle size in the range of 3 μ . For the 5 \times 6 motor approximately 80% of all material was below 1.75 μ and average particle size on a volume basis was approximately 2 μ . In contrast, with the increased particle residence time in the chamber (5 \times 10 motor) approximately 95% of all particles were below 1.75 μ and average particle size on a volume basis was approximately 1.7 μ .

There is no theoretical explanation as yet available for this effect. Moreover, these results are based on a small number of firings at one pressure, and a firm conclusion cannot be drawn without further investigation.

E. Effect of Aluminum Percent in Propellant on Particle Size

Motors containing 16% aluminum in the propellant were fired in the collection tank at various chamber pressures. Aluminum oxide sample analyses from these firings were compared with analyses of samples from motor firings at the same pressures, but containing 12% aluminum in the propellant. Results of the analyses did not show any difference in particle shape, particle size distribution, particle density, or combustion efficiency at any one pressure, by going from 12 to 16% aluminum in the propellant. However, it may be pointed out that higher particle weight fraction in the exhaust gases results in lower efficiency (delivered I_{sp} /theoretical I_{sp}).

F. Effect of Aluminum Particle Size in Propellant on Exhaust Particle Size

To determine the effect of aluminum particle size in the propellant on aluminum oxide particle size distribution, 5 \times 6 motors containing two different grades of aluminum, but the same percentage, in the propellant were fired in the collection tank under identical conditions. The two grades of aluminum used in the propellant were: Alcoa 1230, with a particle size of approximately 15 μ , and MD-105, with a particle size of approximately 5 μ . Results of the microscopic and chemical analyses indicate

³Aeronutronics, a Division of Ford Motor Company, Newport Beach, Calif.

that there was essentially no difference in particle size distribution, particle shape, or particle density. For all practical purposes it can be stated that the size of aluminum particles in the propellant has no effect on aluminum oxide particle size.

G. Effect of Combustion Temperature on Aluminum Oxide Particles

Two different propellant formulations with theoretical flame temperatures of 3629°K and 3300°K were utilized for this series of tests. A basic (5 × 6) motor with a 30-deg nozzle entrance angle was used in the particle collection tests. With propellants having a theoretical flame temperature up to approximately 3300°K, there was no problem of aluminum oxide coating with this motor, and the configurations produced a flat pressure-time curve. With the hotter propellant (3629°K), aluminum oxide coated the convergent and throat section of the nozzle and then sluffed through as large masses of agglomerated particles. The pressure-time trace had a variation of less than 15%. A comparison of microscopic and chemical analysis performed on collected samples from the firings of both propellants under identical conditions indicated that there was no difference in particle shape, character of the X-ray diffraction pattern, aluminum oxide density, or combustion efficiency. As to particle size distribution, comparison was quite difficult because of the large number of agglomerated particles which sluffed through the nozzle in the collection tank. However, after careful investigation, it may be stated that combustion temperature had negligible effect on particle size distribution.

H. Discussion of Extremely Small Particles

The general character of extremely fine particles (in the range of 100 Å to 0.1 μ) is shown in Fig. 15 and 16. These very small particles, even when existing in the 100-Å unit range, still display the strictly spherical character observed in all particles in this study. The extremely small size allows some penetration by the electron beam and permits some insight into the particle character. It can be concluded that particles are not wafer-shaped, as in no case was a particle viewed end-on which displayed anything but a circular cross-section. Since all particles are spherical, the problem then becomes one of defining whether they are hollow spheres or solid spheres. In the case that the spheres are solid, it could be expected that the transmission through the spheres in the central portion would be somewhat longer than in the outer section because of differences in thickness of particle in that region. If the particles are hollow, they would be expected to have a slightly darker region around the periphery, because of greater transmission thickness through an oblique angle at the edge of the sphere, as compared with the normal angle at its center. In some cases observed the latter is true, and most certainly in all cases the transmission in the interior of the sphere is quite uniform. This heavier shading of the periphery is not very easily discerned. If the spheres are hollow, then, the wall thickness must be extremely small. Further insight into the particle character might be available on studying ground portions of extremely small particles, which was not undertaken in this program.

V. CHEMICAL ANALYSIS

Chemical analysis was performed and density determination was made on all the collected samples. Some of the pertinent results are summarized in the following discussion.

For determination of free aluminum, the method used was to treat the samples with strong sodium hydroxide solution and collect any hydrogen liberated. No metallic aluminum was found in any sample.

To determine the soluble aluminum and iron, a weighed sample from each firing, in the as-received condition, was heated to boiling in a beaker with 10% HCl solution. Insoluble residue was filtered off and the filtrate was diluted in a volumetric flask.

Iron was determined on an aliquot of the above filtrate. The iron was first oxidized with KMnO_4 solution and then determined colorimetrically, using the red thiocyanate complex.

Another aliquot was taken for aluminum content determination. Aluminum was separated from other metals with 10% NaOH solution. The filtrate containing aluminum was acidified with HCl and the Al precipitated with NH_4OH solution. The precipitate was filtered off, ignited, and then weighed.

The aluminum content varied in each sample, from a minimum of 0.17% for samples collected from firings at 1000-psi chamber pressure, to 1.0% for samples analyzed from motor firings at 75-psi chamber pressure. Since any aluminum oxide formed in the combustion zone would be insoluble, the aluminum content found may well have come from free aluminum dissolved in HCl. The fact that there was no evidence of metallic aluminum in the residue does not preclude the possibility of some free aluminum having been ejected from the rocket motor during the firing, but probably then dissolved in the HCl, while it resided in the collection tank walls. One conclusion that can be readily drawn from the above analysis is that com-

bustion efficiency is very high even at extremely low chamber pressures.

Another interesting conclusion was drawn from the analysis of the sample collected from the motor firing at 150-psi chamber pressure without any nozzle. From this sample, 0.8% aluminum was extracted with 10% HCl, indicating that almost all the aluminum is burnt in the combustion chamber, and virtually no burning takes place in the convergent section of the nozzle.

For all samples investigated, up to a maximum of 0.6% iron was extracted. It seems probable that the iron came from the corrosion of the stainless steel collection tank.

Various techniques were investigated for determining the densities of the collected aluminum oxide samples. The pycnometer technique, using benzene as the fluid, gave reliable and reproducible results. Since all the samples contained volatiles (basically comprised of H_2O , HCl, and chlorides of Al and Fe), density determinations were made on each sample in the as-received condition, as well as on samples treated to 100°C, 250°C, and 800°C. Densities obtained at 800°C were considered to be the true densities of the aluminum oxide samples, since at this temperature it was possible to eliminate all the volatiles, including chlorides of aluminum and iron. Results obtained from all the samples indicated that the actual density of the collected samples was approximately 85% of the theoretical density for α aluminum oxide. This can be explained by the X-ray diffraction patterns obtained on most of the samples, which indicated that the exhaust particles were a mixture of α and γ aluminum oxide with approximately 1:1 distribution.

Somewhat lower densities were obtained with samples collected from motor firings below 100-psi chamber pressure. As discussed earlier, all the particles in these samples were in the submicron range, and there is a good possibility that some of the very fine particles (below 0.3 μ) might be hollow, which would account for these lower densities.

VI. SUMMARY OF RESULTS

The following conclusions may be drawn from this experimental investigation of a gas-particle system.

1. It has been shown that with aluminized propellants, particle size distribution is pressure-dependent. Lower chamber pressure results in lower particle sizes and vice versa. An empirical relationship is derived giving the average particle diameter D on a volume basis as a function of the chamber pressure P , which is written as

$$\log P = a + b D$$

2. Aluminum percent in propellant, aluminum particle size in propellant, and chamber temperature had virtually no effect on particle size distribution.
3. Nozzle convergent section had no effect on particle size distribution or on the character of X-ray diffraction patterns, but agglomerated particles (due to coating of Al_2O_3 on nozzle walls) increased in number and size when going to steeper nozzle entrance angles.
4. All aluminum oxide particles in every sample existed as near-perfect spheres.

5. Surface replication studies indicated that particle surfaces were smooth and continuous, with no pocks or pores in particles in the range of 0.3μ and above.
6. X-ray diffraction patterns obtained on most of the samples indicated that the exhaust particles were a mixture of α and γ aluminum oxide, with approximately 1:1 distribution.
7. The actual density of the collected samples was approximately 85% of the theoretical density for α aluminum oxide.
8. Combustion efficiency was very high even at extremely low chamber pressure.
9. Samples analyzed from motor firings without any nozzles revealed that almost all the aluminum is burnt in the combustion chamber, and virtually no burning takes place in the convergent section of the nozzle.

It may be concluded that the most effective and direct method to reduce particle sizes is to lower the chamber pressure. Thus for maximum efficiency, upper-stage solid-rocket motors utilizing high-energy aluminized propellants should be designed with very low chamber pressure.

ACKNOWLEDGMENT

The author wishes to express his appreciation to Mr. John Stansel, currently a graduate student at California Institute of Technology, for the design and set-up of the operating procedure for the stainless steel collection tank.

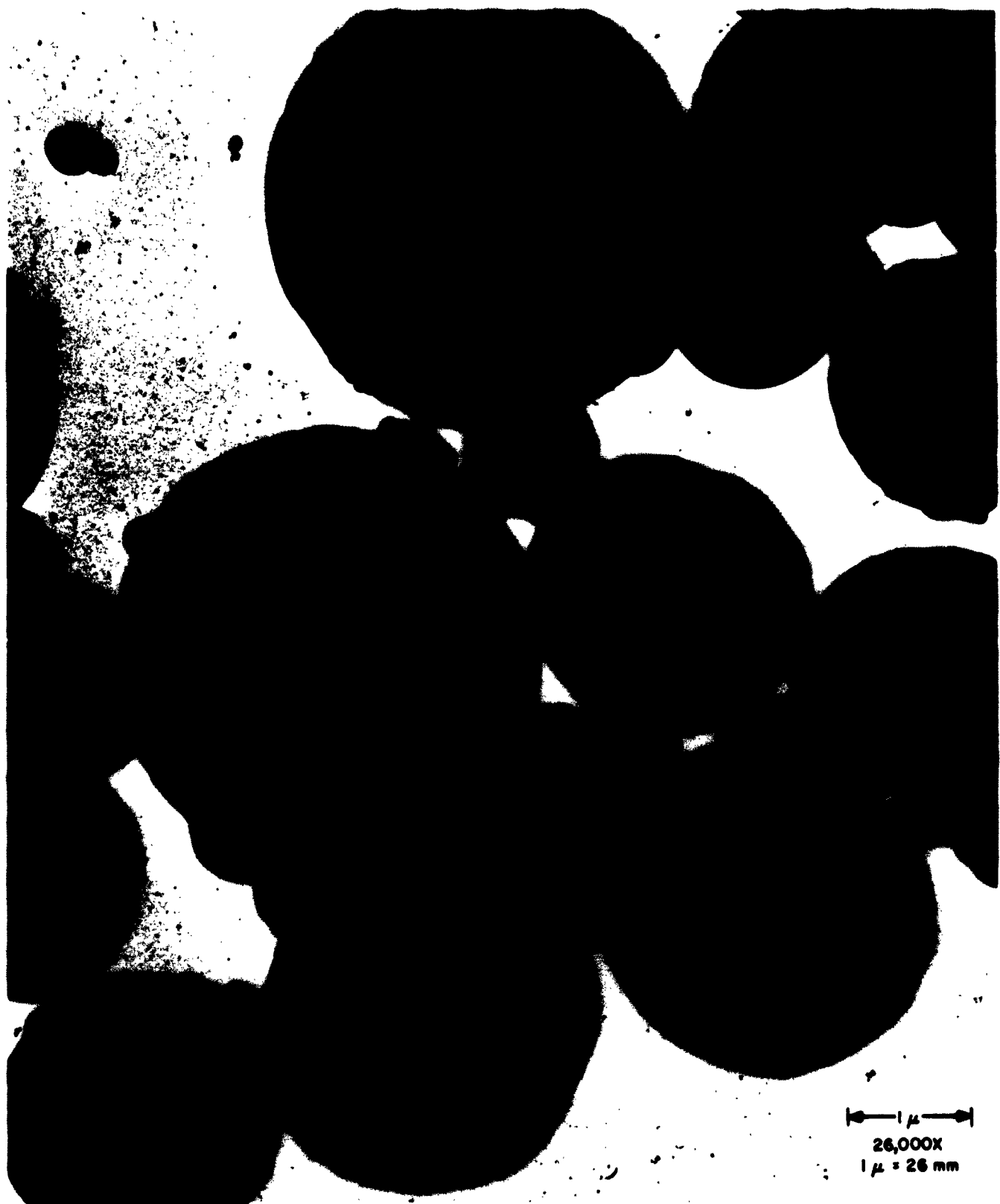


Fig. 5. Micrograph of aluminum oxide sample obtained from motor firing at 1000-psi chamber pressure



Fig. 6. Micrograph of aluminum oxide sample obtained from motor firing at 700-psi chamber pressure



Fig. 7. Micrograph of aluminum oxide sample obtained from motor firing at 500-psi chamber pressure

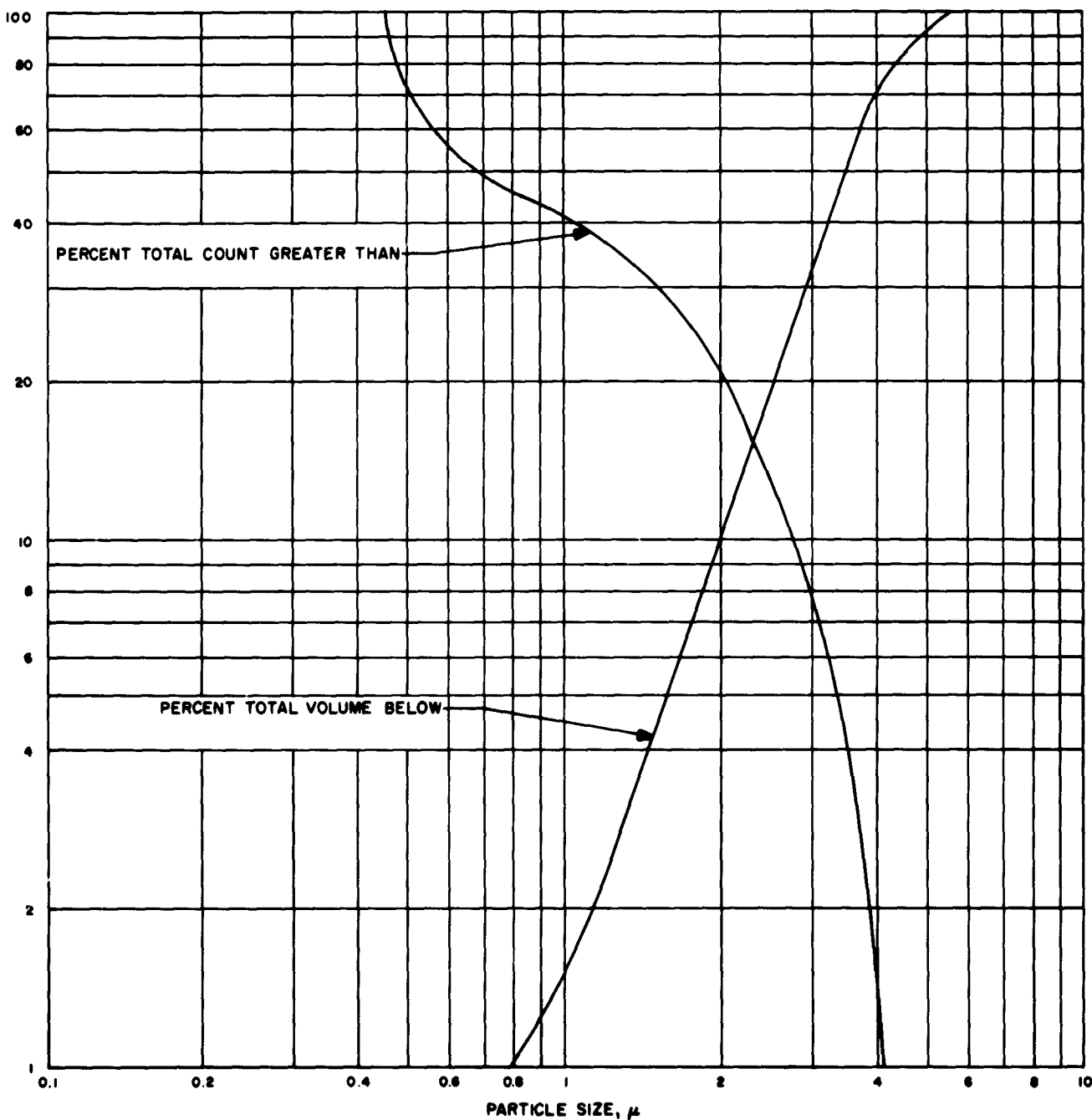


Fig. 8. Plot of percent greater than and percent total volume below vs particle size, of aluminum oxide sample obtained from motor firing at 500-psi chamber pressure

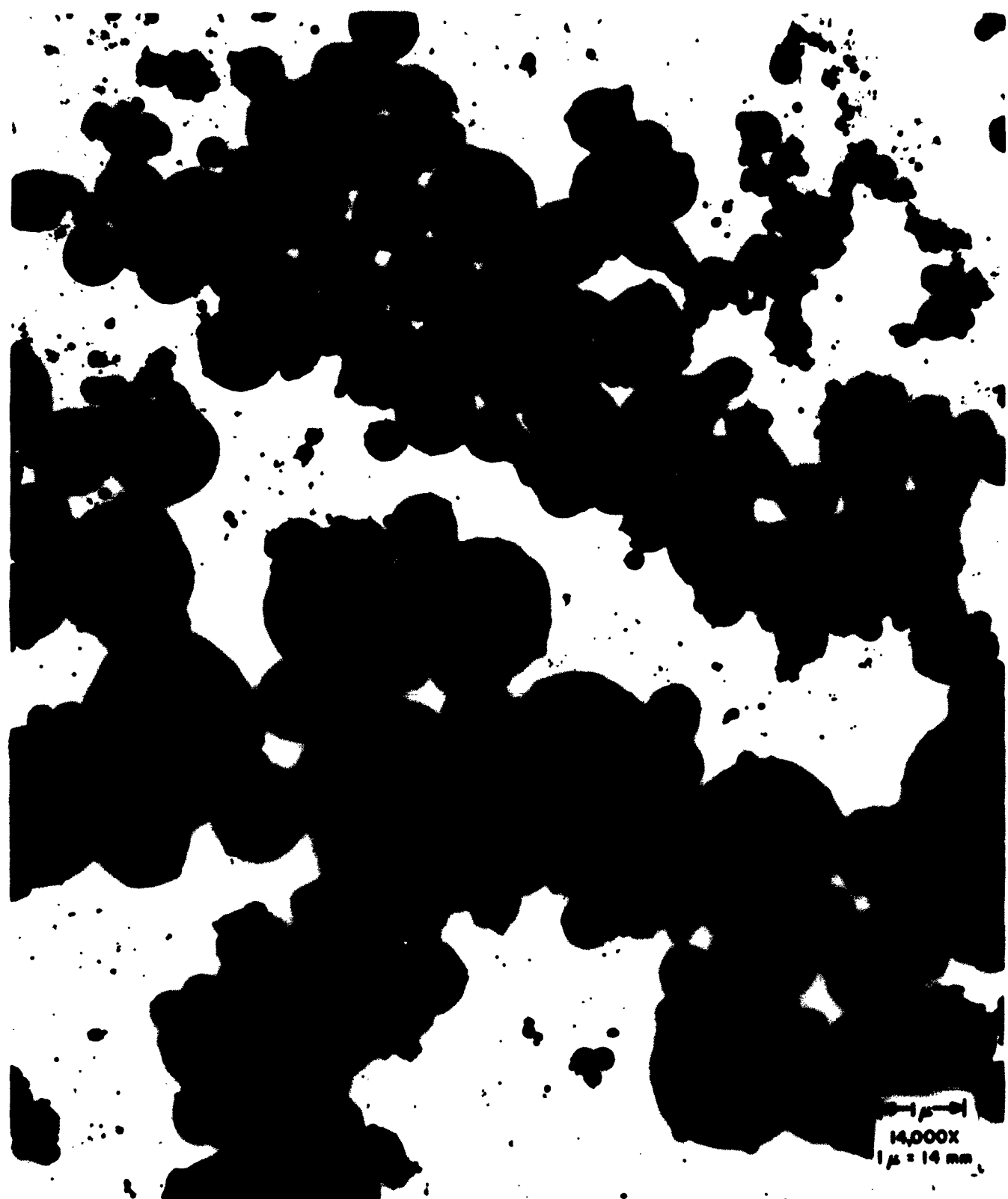


Fig. 9. Micrograph of aluminum oxide sample obtained from motor firing at 365-psi chamber pressure



Fig. 10. Micrograph of aluminum oxide sample obtained from motor firing at 277-psi chamber pressure

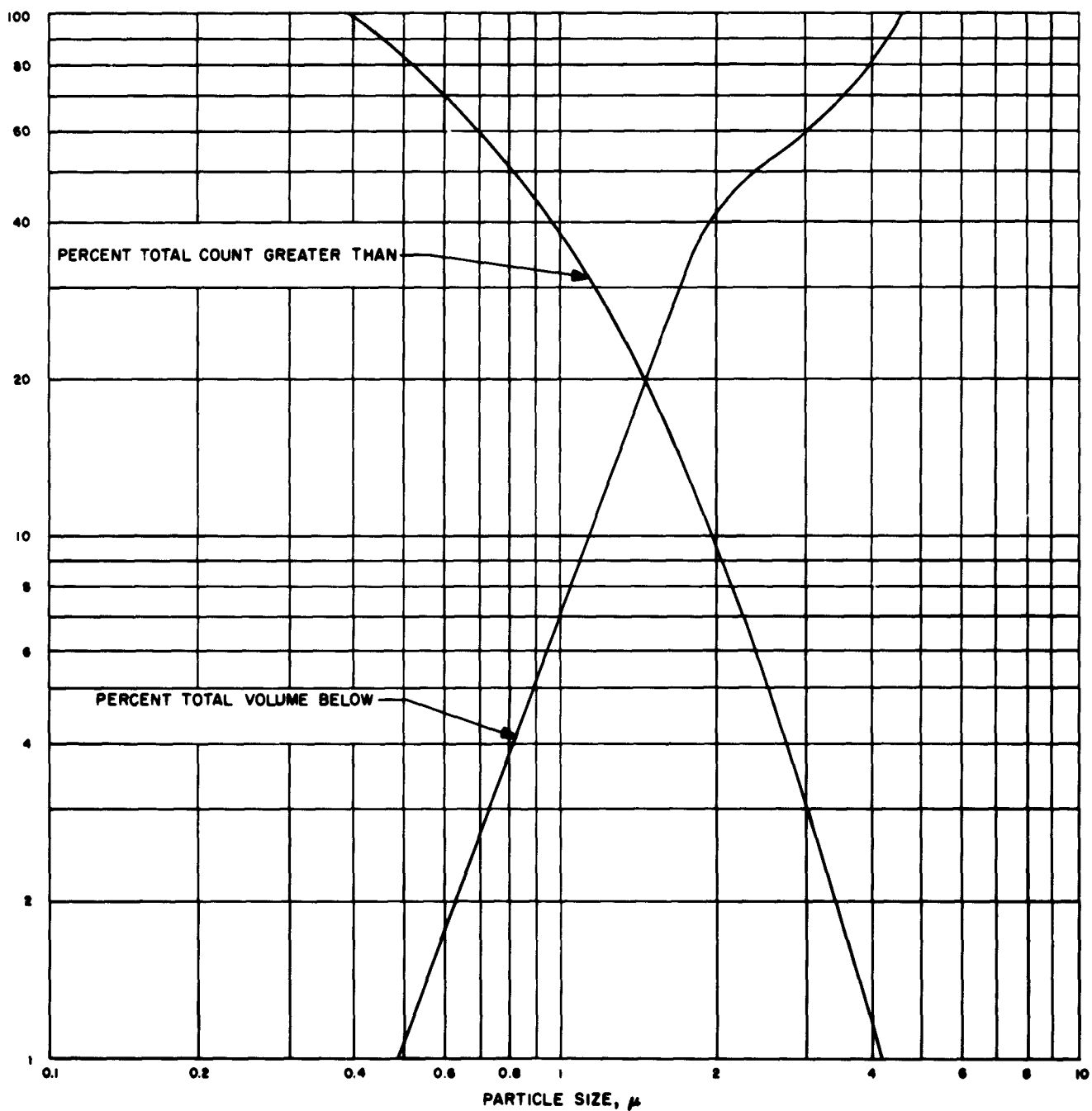


Fig. 11. Plot of percent greater than and percent total volume below vs particle size, of aluminum oxide sample obtained from motor firing at 277-psi chamber pressure

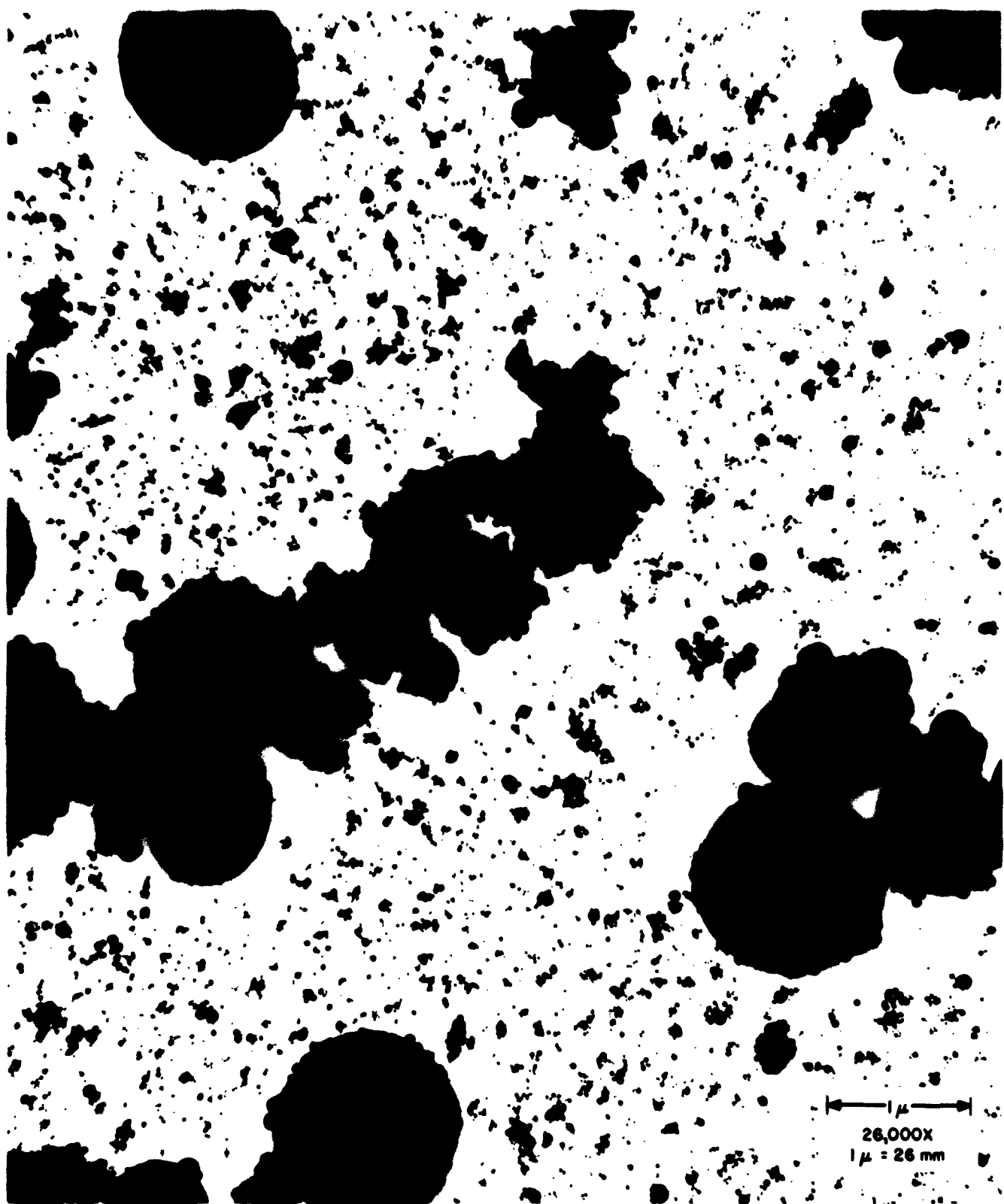


Fig. 12. Micrograph of aluminum oxide sample obtained from motor firing at 200-psi chamber pressure

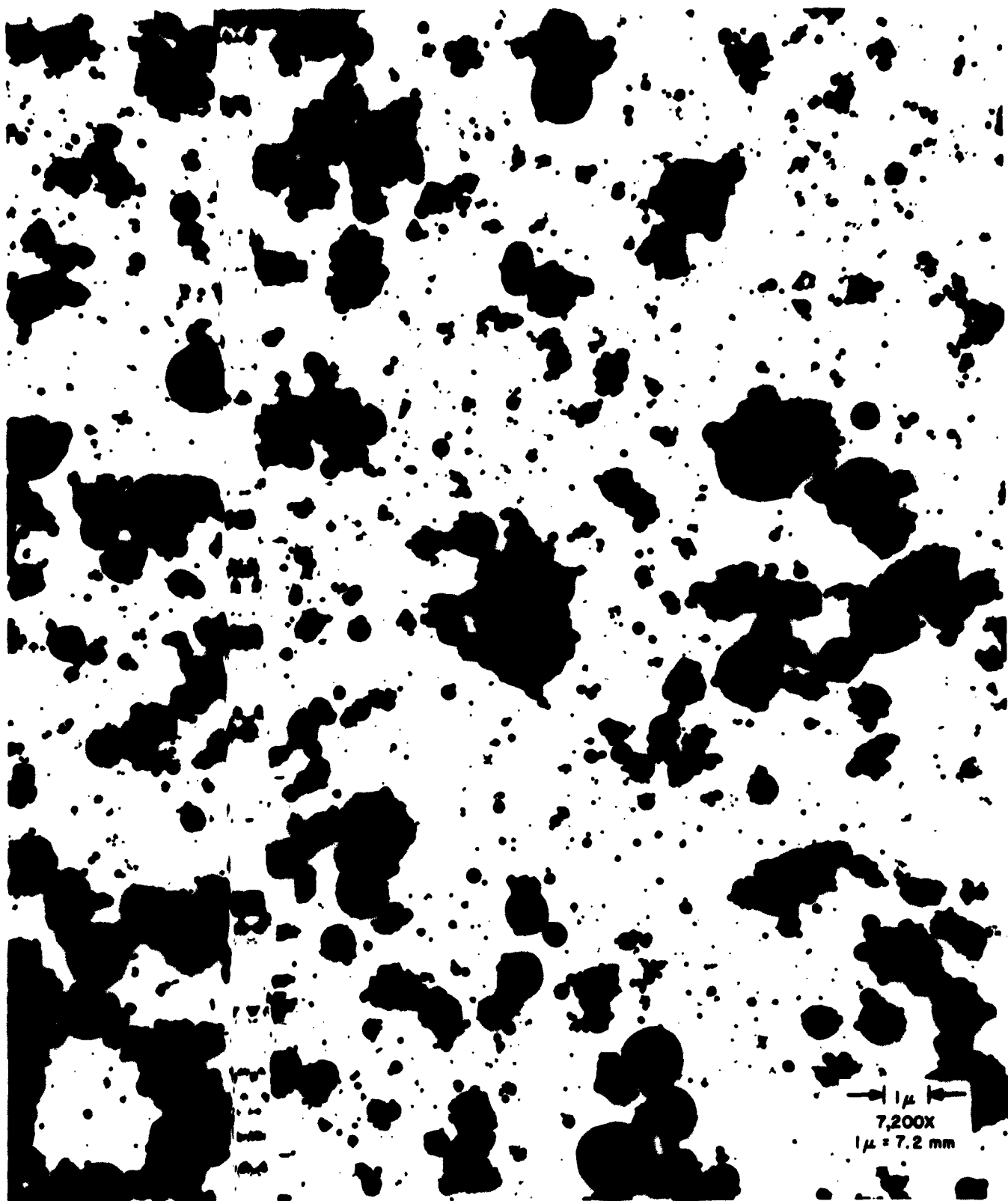


Fig. 13. Micrometeorite oxide sample obtained from motor firing at 150-psi chamber pressure

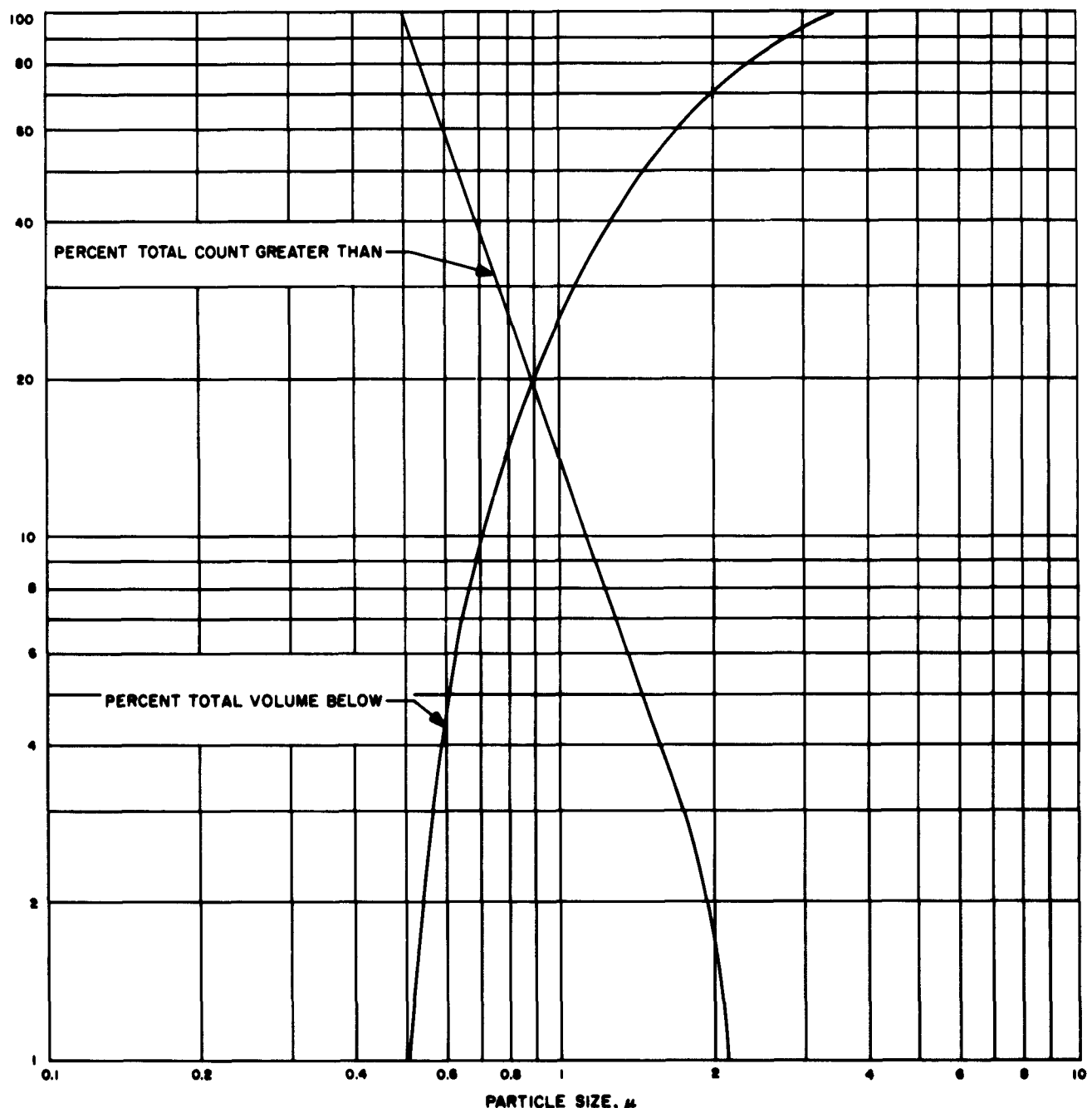


Fig. 14. Plot of percent greater than and percent total volume below vs particle size, of aluminum oxide sample obtained from motor firing at 150-psi chamber pressure

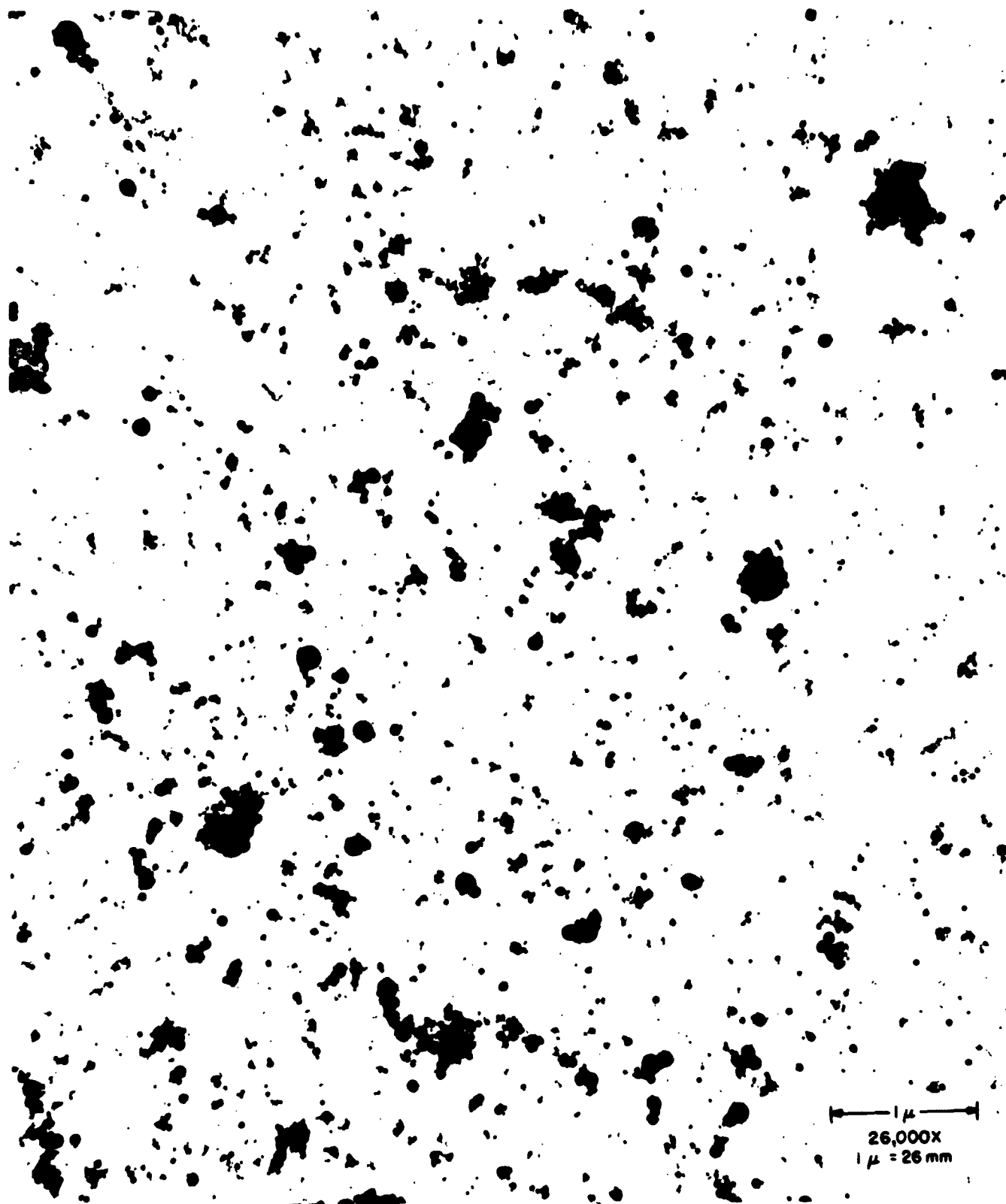


Fig. 15. Micrograph of aluminum oxide sample obtained from motor firing at 75-psi chamber pressure

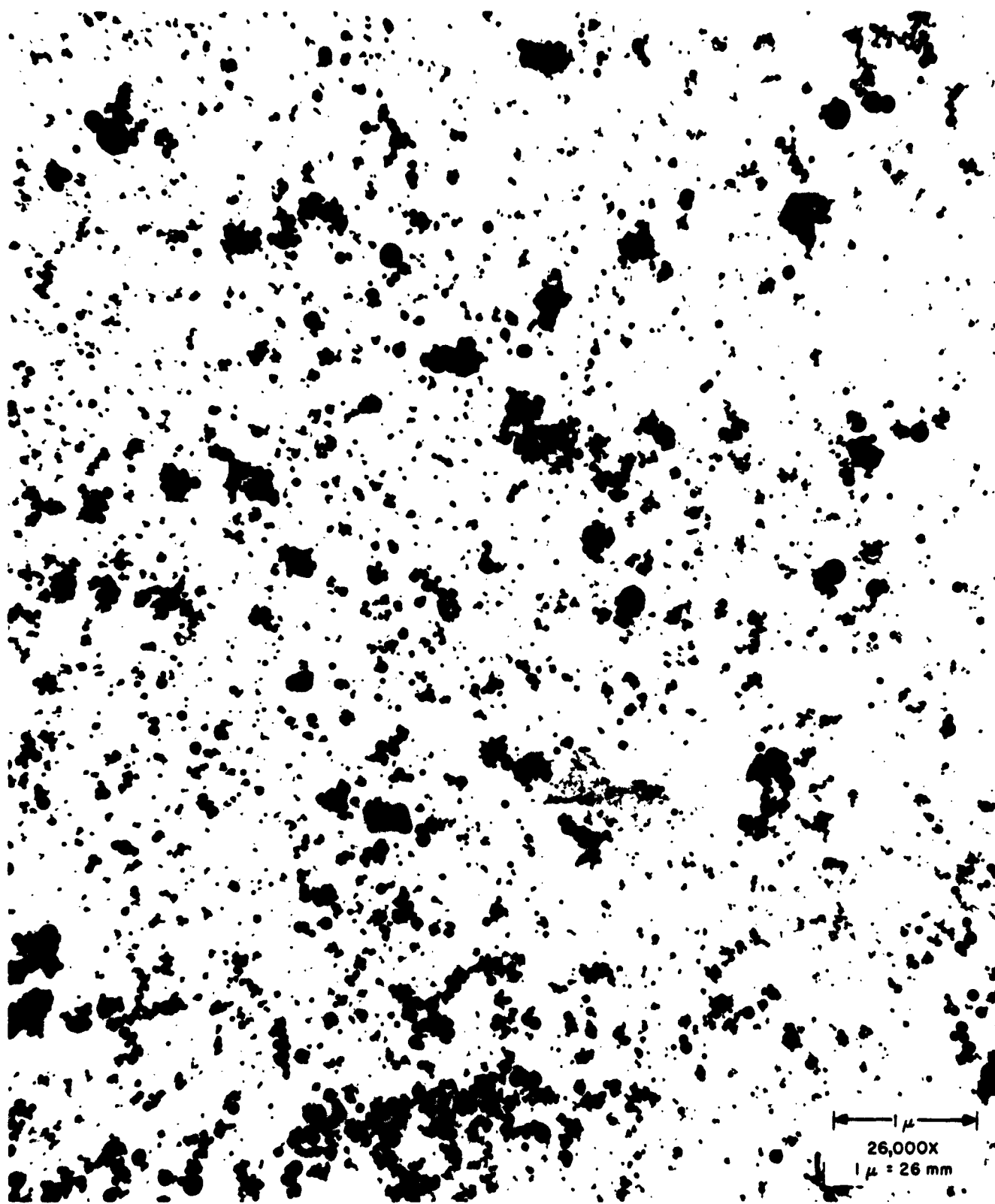


Fig. 16. Another micrograph of aluminum oxide sample obtained from motor firing at 75-psi chamber pressure

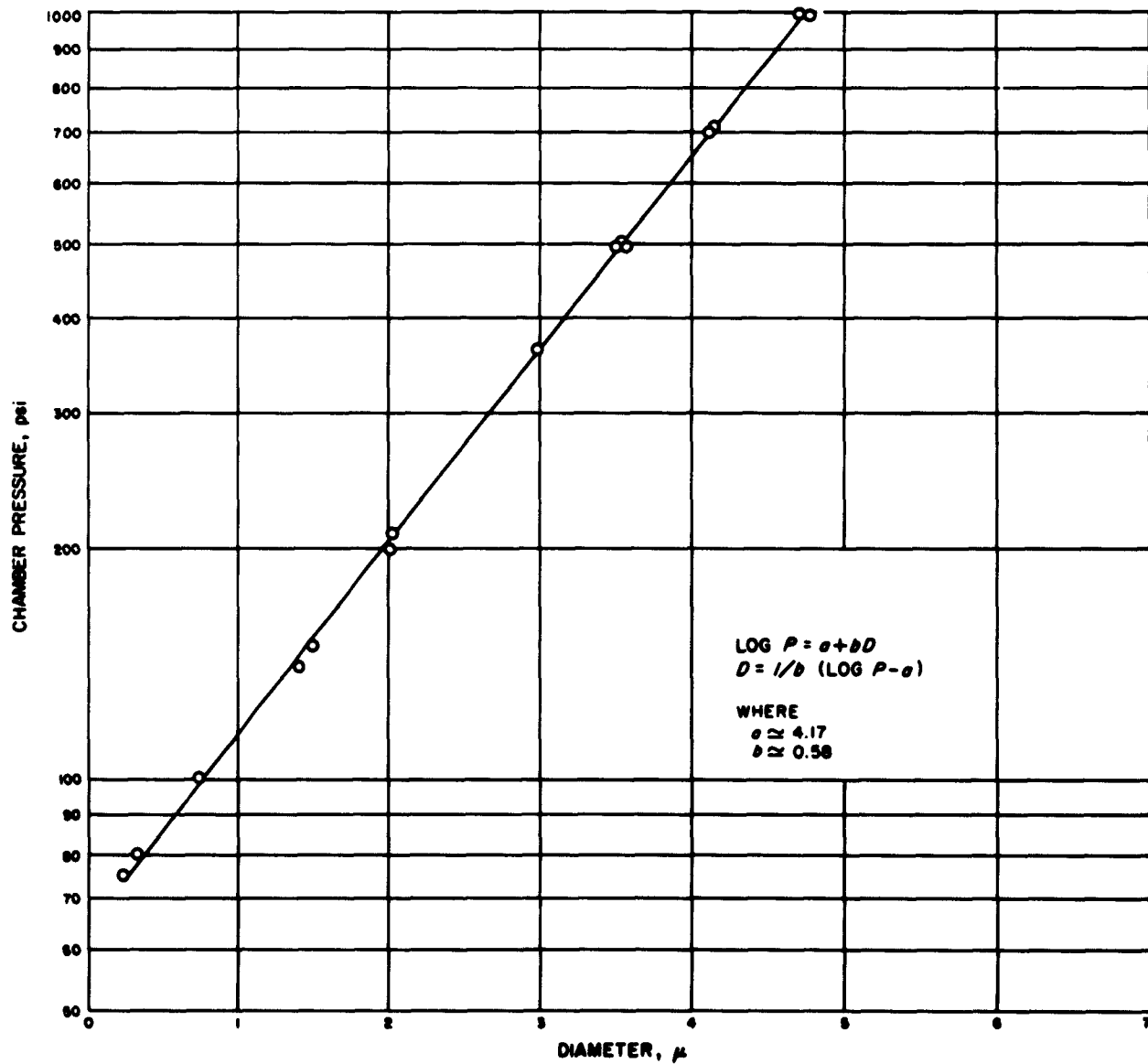


Fig. 17. Plot of chamber pressure vs average particle size by volume

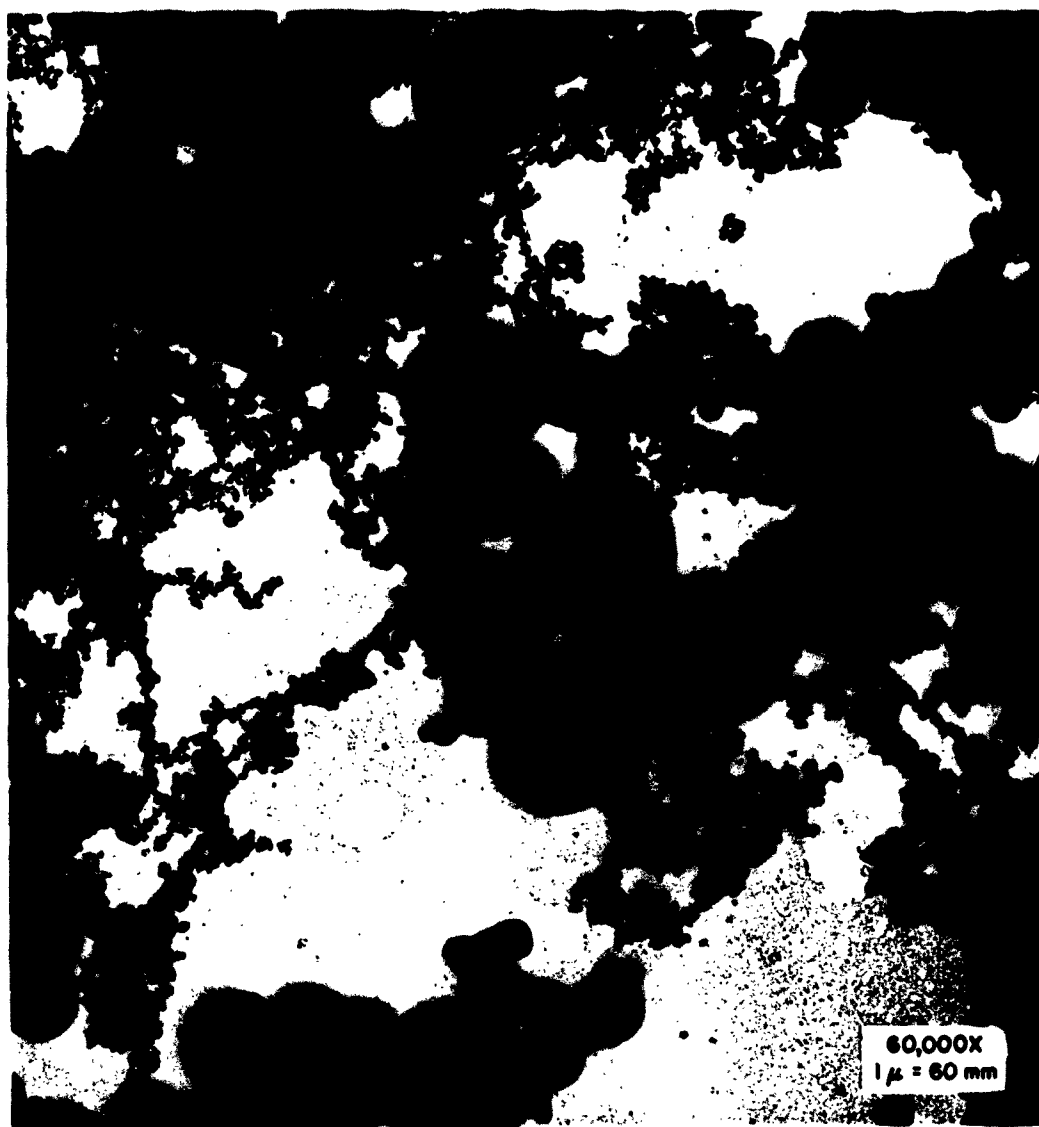


Fig. 18. Micrograph of aluminum oxide sample obtained from motor firing at 150-psi chamber pressure and without any nozzle (micrograph supplied by Aeroneutronics, a Division of Ford Motor Company)